

Ph 442 Solutions for Problem Set 3

1. a) The binding energies of some of the elements with mass 56 are given in the table below, with the numbers taken from the atomic mass data given on the National Nuclear Data Center website and stability taken from the Chart of the Nuclides (stability was not clearly indicated in the mass table). The most tightly bound nucleus with mass 56 is ^{56}Fe and it is the only stable nucleus with

Table 1: Some Nuclei with Mass 56

Z	24	25	26	27	28
Element	Cr	Mn	Fe	Co	Ni
Binding E/A (keV)	8723.191	8738.300	8790.323	8694.817	8642.709
uncertainty BE/A	0.033	0.012	0.012	0.038	0.198
stable?	N	N	Y	N	N

that mass. The table below gives similar data for some elements with mass 58. Both ^{58}Fe and ^{58}Ni are stable.

Table 2: Some Nuclei with Mass 58

Z	24	25	26	27	28	29	30
Element	Cr	Mn	Fe	Co	Ni	Cu	Zn
Binding E/A (keV)	8641.290	8698.010	8792.221	8738.947	8732.041	8570.869	8395.926
uncertainty BE/A	3.499	0.517	0.012	0.022	0.011	0.027	0.862
stable?	N	Y	N	Y	N	N	

b) While ^{56}Fe and ^{58}Fe are among the most bound nuclei, the nucleus ^{62}Ni is the most tightly bound with a binding energy per nucleon of 8794.549 ± 0.010 keV. It has a 28 protons, which produces a closed shell. This nucleus is not produced in abundance in core-collapse and Type Ia supernova because the conditions during explosive nucleosynthesis favor the slightly less massive and less neutron rich ^{56}Ni .

c) The most bound nucleus with equal numbers of protons and neutrons is ^{56}Ni .

d) The chart of the nuclides with $N = 78$ to 83 and $Z = 53$ to 58 is given below. The path of the s process is to the right (adding a neutron) until reaching an unstable nucleus. The unstable nucleus beta decays to produce the element up and to the left (one neutron is converted to a proton). Beta decays continue until reaching a stable nucleus, where the rightward motion resumes. In the r process, nuclei are driven far from the valley of beta stability by the rapid addition of neutrons.

These nuclei subsequently beta decay along diagonals until reaching a stable nucleus. A nucleus cannot be created by the s process if there is an unstable nucleus to the left of it in the chart. A nucleus cannot be created by the r process if it is shielded by a stable nucleus below and to the right of it along the diagonal. Note that some nuclei are not produced by either the r or the s process. Some other nucleosynthetic mechanism (involving the addition of protons or neutrino interactions) must produce these nuclei.

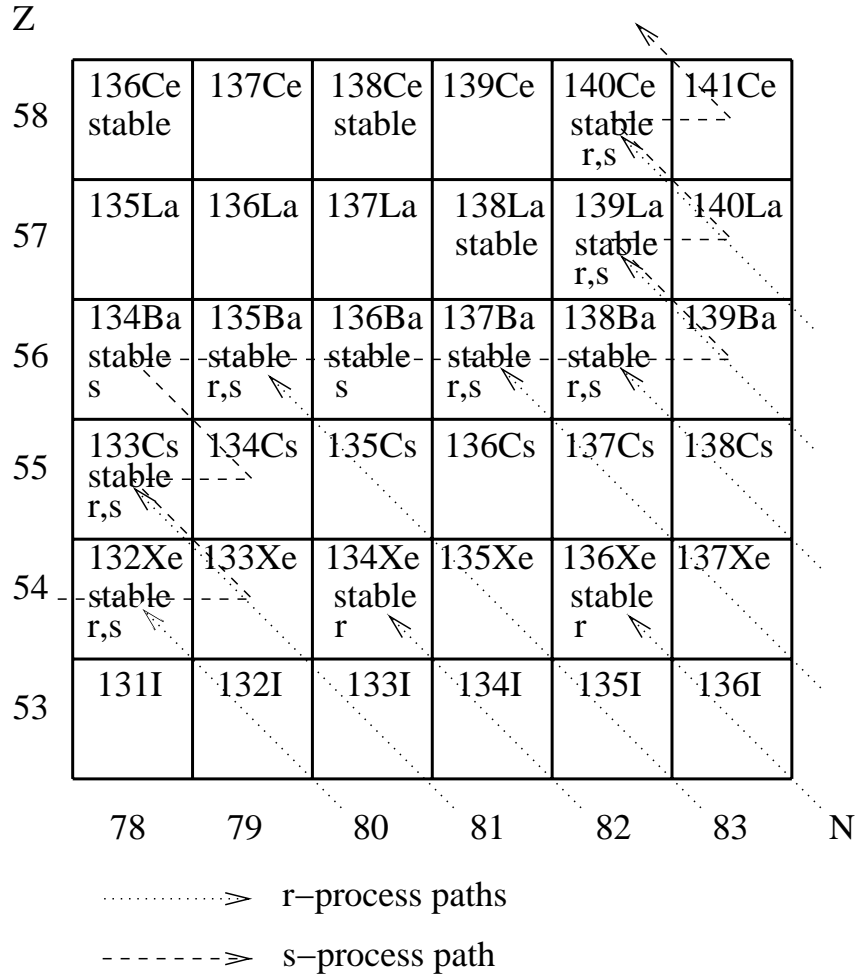


Figure 1: Chart of the nuclides with $N = 78$ to 83 and $Z = 53$ to 58 .

e) The isotope ^{139}La has 82 neutrons, which is the number that creates a closed shell. Closed shells are particularly stable, so we would expect the cross-section for adding an additional neutron to be small. Thus, the s process will feed nuclei into ^{139}La , but will be slow to move them on to more massive nuclei. Thus, nuclei will pile up in ^{139}La and it will should have a high production by the s process.

2. Any detector which records the arrival of individual photons will become inaccurate if the arrival rate is too high. The standard physical model for this problem is to assume that, after the detection of a photon, there is a time interval Δt during which the detector is not functioning (*i.e.*, “dead”).

If R is the observed count rate, then in a time T the average number of observed counts is RT and the average length of time that the detector is dead during T is $RT\Delta t$. The true count rate, R' , is larger than R by the ratio of T to the time during which the detector was “live” during T . Thus,

$$R' = \frac{T}{T - RT\Delta t} R = \frac{R}{1 - R\Delta t}. \quad (1)$$

If $R = 100$ counts s^{-1} and $\Delta t = 1$ ms = 10^{-3} s, then

$$R' = \frac{100 \text{ counts s}^{-1}}{1 - (100 \text{ counts s}^{-1})(10^{-3} \text{ s})} = \frac{100 \text{ counts s}^{-1}}{1 - 0.1} = 111 \text{ counts s}^{-1}. \quad (2)$$

3. This problem examined the expected photon count rates from various sources for different satellites and detectors.

a) An approximate method to convert an energy flux to a photon flux is to divide by the energy of a photon near the middle of the energy bandpass. A more precise calculation would be to calculate the average photon energy in the bandpass, but this requires knowing the spectrum of the source (*i.e.*, the flux of photons as a function of energy). An energy of 1 eV is 1.602×10^{-12} erg, so a 4 keV photon has an energy of 6.41×10^{-9} erg. Thus, the flux of photons from Sco X1 is $(3 \times 10^{-7} \text{ erg cm}^{-2} \text{ s}^{-1}) / (6.41 \times 10^{-9} \text{ erg}) = 47$ photons $\text{cm}^{-2} \text{ s}^{-1}$. Multiplying this flux by the effective area of the Uhuru detector, 280 cm^2 , yields the expected count rate of 1.3×10^4 counts s^{-1} . Doing the same calculation for one unit (PCU) of the proportional counter array (PCA) of RXTE, with an effective area of 920 cm^2 , gives a rate of 4.3×10^4 counts s^{-1} . These results and those for the other three sources are given in the table below.

Table 3: Count Rates for Uhuru and RXTE

Source	Sco X1	Crab SNR	Perseus Cluster	QSO 3C273
flux ($\text{erg cm}^{-2} \text{ s}^{-1}$)	3×10^{-7}	2×10^{-8}	1×10^{-9}	8×10^{-11}
flux (photons $\text{cm}^{-2} \text{ s}^{-1}$)	47	3.1	0.16	0.012
Uhuru rate (photons s^{-1})	1.3×10^4	8.7×10^2	44	3.4
RXTE rate (photons s^{-1})	4.3×10^4	2.9×10^3	1.5×10^2	11

Note that the effective area of RXTE was not dramatically larger than that of Uhuru (although RXTE had five PCUs that operated simultaneously). Other important contributors to the gain in sensitivity in going from Uhuru to RXTE were i) the ability of RXTE to do pointed observations *versus* the continual scanning of Uhuru; ii) the better angular resolution of the RXTE collimators (1 degree *versus* 5 degrees), which reduces the background from other sources; and iii) the lower background of the RXTE PCUs, the same 10 counts s^{-1} as Uhuru despite the larger effective area.

The important quantity for assessing deadtime is $R\Delta t$, where R is the rate and Δt is the deadtime. For Sco X1 and RXTE this product is $(1.3 \times 10^4 \text{ photons s}^{-1})(8.8 \times 10^{-6} \text{ s}) = 0.38$. Since the result is a significant fraction of 1.0, the answer is: yes, deadtime corrections will be significant.

b) If the source rate is R and the background rate is B , then the signal-to-noise ratio for an observation of length t is

$$\frac{S}{N} = \frac{Rt}{\sqrt{Rt + Bt}} = \frac{R}{\sqrt{R + B}}\sqrt{t}. \quad (3)$$

and the length of time needed to achieve a particular S/N is

$$t = \frac{R + B}{R^2} \left(\frac{S}{N}\right)^2. \quad (4)$$

With $R = 3.4$ counts s^{-1} for Uhuru observing 3C273 and $B = 0$ counts s^{-1} , the time to achieve $S/N = 100$ is

$$t = \frac{3.4}{3.4^2}(100)^2 = 2.9 \times 10^3 \text{ s}. \quad (5)$$

With the real background of 10 counts s^{-1} , the time is

$$t = \frac{3.4 + 10}{3.4^2}(100)^2 = 1.2 \times 10^4 \text{ s}. \quad (6)$$

Thus, the background greatly increases the amount of observing time needed. The flux from the quasar 3C273 was only measured with an accuracy of about 7% with Uhuru, even after combining all of the data from the mission.

c) With a photon flux of 0.012 photons $\text{cm}^{-2} \text{ s}^{-1}$ from 3C273 and an effective mirror area of $(350 \text{ cm}^2)/2 = 175 \text{ cm}^2$ for the Einstein IPC, the expected rate is 2.1 counts s^{-1} . If the background of 10 counts s^{-1} is uniformly spread over the $75' \times 75'$ area of the *imaging* IPC detector, then only a small fraction of those background counts will be in the vicinity of the approximately $1'$ diameter source. Quantitatively, the fraction of background counts that will be coincident with the source is $\pi(0.5')^2/(75' \times 75') = 1.4 \times 10^{-4}$. Thus, the background rate for the source is only $(10 \text{ counts s}^{-1})(1.4 \times 10^{-4}) = 1.4 \times 10^{-3}$ counts s^{-1} . This rate is negligible compared to the source rate of a few counts s^{-1} . This example shows the ability of imaging detectors to greatly reduce the effect of the background.

d) The biggest problem that students encountered with this part was that numbers in scientific notation had to be entered in the format 8.0e-11 for the flux and 1.8e20 for N_H . One enterprising student found that 0.00000000008 also worked, though it seems to give slightly different numerical results for some reason. The values that I got from the WEBPIMMS tool were as follows.

- Einstein IPC: 4.228 counts s^{-1} ; this is a factor of two larger than our calculated value, probably due to the different energy bandpass (0.4 – 4.0 keV), though a larger mirror effective area is another possibility.
- RXTE: 9.456 counts s^{-1} for one PCU; this is within 16% of our calculated rate.
- Chandra ACIS-I: 13.9 counts s^{-1} ; though “pile-up” is important for the standard CCD exposure time. In other words, many photons would hit the same CCD pixel during the usual 3.2 s exposure time and be counted as a single detection.

- XMM PN: 41.8 counts s^{-1} ; pile-up is again significant. The WEBPIMMS output provides results for observing modes that read out just a portion of the CCD and so reduce the exposure time.

3. Consider an atom with nuclear charge Ze and neglect the effects on the electron Hamiltonian of spin, special relativity, and the extended size of the nucleus. If the potential is of Coulomb form (*i.e.*, the interactions between electrons can be ignored or treated as simply reducing the charge of the nucleus by shielding) then we have the Bohr model of the atom and the energy levels are

$$E_n = -\frac{m_e e^4 Z^2}{2\hbar^2} \frac{1}{n^2} = (-13.6 \text{ eV}) Z^2 \left(\frac{1}{n^2} \right), \quad (7)$$

where $n = 1, 2, \dots$. For iron, $Z = 26$ and $E_n = (-9.19 \text{ keV})/n^2$.

- The $K\alpha$ line arises from the transition between $n = 1$ and $n = 2$. The energy difference is $(9.19 \text{ keV})(1/1^2 - 1/2^2) = 6.90 \text{ keV}$. The true value is 6.97 keV because of the combined effects of spin-orbit coupling, relativity, and a field-theoretic treatment of the radiation field. Some students noted Moseley's law from the early 1900's. This empirical law resulted from studying the emission of X-rays (probably from neutral atoms) and was important in the development of the theory of atomic structure. The presence of other electrons changes the electronic energy levels (see the answer to c)).

- The energy of the iron K edge is just the energy of the $n = 1$ level: 9.19 keV.

- If the atom has two electrons, then the repulsive force between the pair of electrons and the shielding of the charge of the nucleus by the other electron will both act to reduce the energy needed to remove one electron. Thus, the energy of the K edge will be smaller in this case.

We will encounter the case where X-rays are absorbed by neutral iron atoms, resulting in K-edge absorption and $K\alpha$ fluorescent emission as less-bound electrons drop down to fill the K-shell state. The effect of the additional electrons is to produce a $K\alpha$ doublet (two lines) at 6.391 and 6.404 keV and a K edge at 7.111 keV.

- The reasons that Fe $K\alpha$ emission is so strong have to do with the large charge on its nucleus. One reason is that the photoelectric absorption cross-section increases with Z proportional to Z^5 for hydrogenic atoms and proportional to Z^4 for neutral atoms (page 5 of the Garmire notes). Thus, an iron atom is more likely than, say, a carbon, nitrogen, or oxygen atom to remove a K-shell photon by the absorption of an x-ray photon, with the possible subsequent emission of a $K\alpha$ photon. A second reason for $K\alpha$ emission being common has to do with how the K-shell hole is filled. The two possibilities are the emission of a photon (fluorescence) or the emission of an Auger electron. For high Z , fluorescent emission is favored over the Auger process. For L- to K-shell transitions, the fraction of atoms de-exciting by the emission of a photon is empirically given by $Z^4/(Z^4 + 10^6)$ (page 6 of the Garmire notes). Thus, iron produces more fluorescent emission per photoionization than does C, N, or O.